33rd Annual International Conference of the IEEE EMBS
Boston, Massachusetts USA, August 30 - September 3, 2011

Two new stable anatomical landmarks on the central sulcus: definition, automatic detection, and their relationship with primary motor functions of the hand

Olivier Coulon Fabrizio Pizzagalli Grégory Operto Guillaume Auzias Chantal Delon-Martin Michel Dojat

***Abstract*— We present a method to automatically detect two new stable anatomical landmarks L_1 and L_2 on the Central Sulcus (CS). Those landmarks are shown to be representative of the Central Sulcus morphology and linked to the functional primary motor area of the hand. Detection is performed after introducing a new morphological characteristic, the sulcal profile. We show that when matching explicitly L_1 and L_2 across individuals the inter-subject matching of the central sulcus anatomy is improved , as well as the inter-subject matching of the primary motor area of the hand. This opens possibilities for morphological studies of the CS, more precise functional studies of primary motor function, and a better understanding of motor representations along the CS.**

I. INTRODUCTION

In human, the precise functional organisation of the primary motor cortex (M1) is largely unknown. Knowledge about its anatomical and functional organisation in healthy subjects could help understanding deficiencies related to specific pathologies (e.g Parkinson's disease) or cortical plasticity after surgery or amputation (phantom member representation). Structural and high resolution functional MR imaging are suitable non-invasive modalities for investigating hand representation in M1. M1 lies just anterior to the central sulcus (CS) and extends across the precentral gyrus. It appears that a part of the CS is shaped like an inverted omega or epsilon in the axial plane and like a hook in the sagittal plane (knob-like structure, Fig. 1). This 'knob' is a reliable landmark for identifying M1 [1]. In group studies, a perfect alignment of all individual "knobs" is a prerequisite for a robust detection of statistically significative cortical activation following hand movement. Clearly, such a registration is hampered by the high individual variability of the 'knob' structure (as shown on various indidual CS morphologies in Fig. 3). Another more local landmark associated to the hand representation in M1 is the 'Pli de passage fronto-parietal moyen' (PPFM, [2]), a buried gyrus associated to a local decrease of the CS depth [3]. Its detection is awkward and also suffers from the high inter-subject variability. In this paper, we propose the definition of two new anatomical landmarks of the CS. We introduce a morphological characteristic of the CS, the *sulcal profile*, and show that the two landmarks can be robustly detected using the sulcal profile. These landmarks are used to define a referential on the CS common to several individuals. We show that it provides a relevant anatomical inter-subject matching and that the hand representation in M1 is stable in this referential.

In the next section, we present the methods we proposed to extract the sulcal profile, detect the two landmarks and reparameterize the CS. Then we present experiments, for a group of 10 healthy subjects with anatomical and functional data, and the results we obtain..

II. METHODS

A. Sulcus Parameterization

In [3], [4] a method was presented to parameterize the CS and perform depth measurements. In this paper, we propose an extension to this method to define a CS-based referential and use it to analyze functional data. We briefly recall the idea behind the parameterization and the depth curve extraction. From T1 MR images, we extract the CS as a 3D mesh, by using BrainVisa[1]. On this mesh, the two extremities and the two ridges, at the fundus of the sulcus and at the convex hull, are automatically extracted. Using these landmarks, two coordinate fields are computed on the sulcus that indicate the depth between the two ridges (x coordinate) and the longitudinal position between the two extremities (y coordinate). For each value of $y \in [0; 100]$, we estimate the depth at this position by measuring the length of y iso-parameter lines. Depth as a function of the y position can then be computed, as shown in Fig. 1.

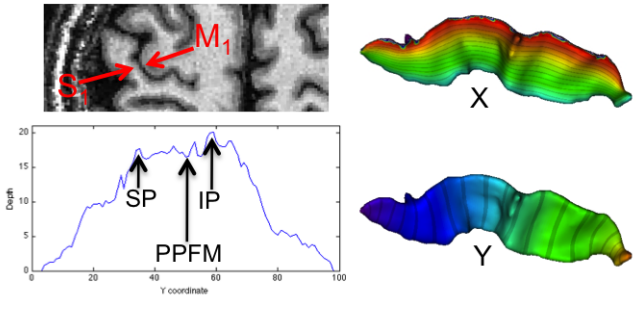

Fig. 1. The central sulcus 'knob' area with primary motor (M1) and sensori (S1) areas (top left), a CS mesh with X and Y coordinate field (right, with iso-parameter lines in dark) and depth curve (bottom left)

O. Coulon and G. Auzias are with Laboratoire des Sciences de l'Information et des Systèmes, UMR CNRS 6168, Marseille, France, olivier.coulon@univmed.fr

F. Pizzagalli, C. Delon-Martin and M. Dojat are with Institut des Neurosciences de Grenoble, Grenoble, France,

G. Operto is with Neurospin Center, CEA, Gif-Sur-Yvette, France,

[1]http://brainvisa.info

It has been shown that the parameterization available via the x and y coordinate fields provides a good inter-subject matching for morphological statistical studies. In particular, depth curves have been showing left-right asymetries related to handedness depth asymetries in humans [3], as well as in chimpanzees [4]. The depth curve has also been used to localize the PPFM, defined as the point of least depth between the inferior peak (IP) and superior peak (SP), as illustrated in Fig. 1. Although visible on an average depth curve computed from a group of subjects ([3], [4] and Fig. 5), the PPFM is sometimes difficult to detect on individuals, as shown in Fig. 3. Furthermore, although it is thought to be related to hand-related primary motor area, to what extent this statement is true is not very well known. This motivates the definition and detection of mode robust anatomical landmarks common to individuals.

B. A new morphological characteristic: the sulcal profile

The CS clearly has a main dorso-ventral direction (∼the direction along the y coordinate), and apart from depth variations, its morphology can be described in terms of how much it bends along this direction. We introduce the *sulcal profile* in order to provide such information. The sulcal profile aims at measuring shape variations along the sulcus (y coordinate) in terms of deviation from the inertia plane, i.e. the plane that defines the main orientation of the sulcus. For a given sulcus mesh, defined as a vector of nodes $\mathbf{S} = (\mathbf{n}_i)_{i=1...N}$, with $\mathbf{n}_i = (n_{xi}, n_{yi}, n_{zi})^T$ the nodes of the mesh, let us define the centered mesh $\mathbf{S_c} = (\mathbf{n}_i - \overline{\mathbf{n}})$, with $\overline{\mathbf{n}}$ the barycenter of $\mathbf{S}$. We then compute $\mathbf{A} = \mathbf{S_c}.\mathbf{S_c}^T$. After diagonalization, let $\mathbf{u}_1$, $\mathbf{u}_2$, and $\mathbf{u}_3$ be the 3 eigenvectors of $\mathbf{A}$ ordered by decreasing eigenvalue. The inertia plane (Fig. 2) is defined by $(\overline{\mathbf{n}}, \mathbf{u}_1, \mathbf{u}_2)$, and the signed distance of any node $\mathbf{n}_i$ to this plane is :

$$d_i = (\mathbf{n}_i - \overline{\mathbf{n}}).\mathbf{u}_3 \quad (1)$$

Fig. 2 shows a color representation of d_i at every node of a sulcus. At each position y, the sulcal profile function is then defined as the average value of d_i on the mesh at position y (i.e. along the y iso-parameter line). A sulcal profile as a function of y is presented on Fig. 2, showing how it represents shape information along the sulcus.

C. Automatic detection of anatomical landmarks and sulcal reparameterization

The central sulcus has been defined as being omega-shaped or in certain cases epsilon-shaped [1]. In both cases, when following the sulcus from the dorsal to the ventral extremities (y increasing), in the 'knob' area it first bends to an extremum in the posterior direction before coming back to another extremum towards the anterior direction. This shape corresponds to a large minimum of the sulcal profile, followed by a local maximum, as can be observed on Fig. 2 and 3. The latter clearly shows that the sulcal profile provides a more consistent information across subjects than the depth curve. Therefore, we propose to define two landmarks on the y axis, corresponding to the position of those two

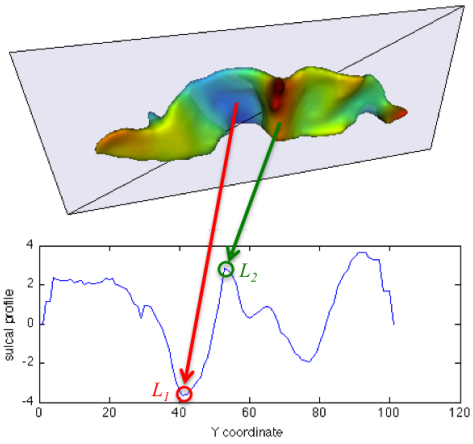

Fig. 2. Sulcus with inertia plane and color-coded (from negative in blue to positive in red) distance-to-plane information (top) and corresponding sulcal profile curve (bottom), with the two anatomical landmarks L_1 and L_2.

extrema. The first landmark L_1 is defined at the position y_1 corresponding to the global minimum of the sulcal profile in the inferior two thirds of the central sulcus ($y \in [0; 66]$). The second landmark L_2 is then defined at the position y_2 corresponding to the first local maximum of the sulcal profile after y_1. Prior to the detection, the sulcal profile is smoothed with a small Gaussian smoothing of variance $\sigma^2 = 3$ in order to remove spurious local extrema due to noise. Fig. 3 shows an example on the left central sulcus of four subjects, with the smoothed sulcal profiles and the automatically detected landmarks, illustrating the robustness of their definition.

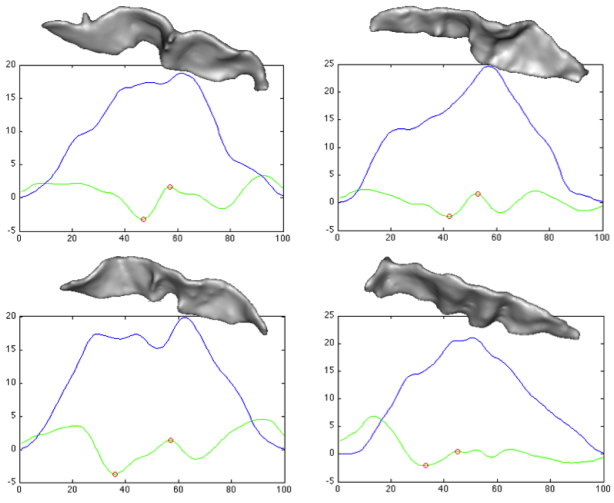

Fig. 3. Smoothed depth (blue) and sulcal profile (green) of 4 subjects with two landmarks automatically detected for each subject (red circles)

A new parameterization is computed by rescaling the Y coordinate in a piecewise linear fashion, such as to match exactly the coordinate of the two anatomical landmarks L_1 and L_2 across subjects. For a given subject, let $\overline{y_1}$ (resp. $\overline{y_2}$) be the mean of y_1 (resp. y_2) across subjects. In order to minimize metric distortions after reparameterization, we

therefore perform the following rescaling:

$$\begin{aligned} &\text{if } y \leq y_1, && y_{new} = \frac{\overline{y_1}}{y_1}.y, \\ &\text{if } y_1 < y \leq y_2, && y_{new} = \frac{\overline{y_2}-\overline{y_1}}{y_2-y_1}.y + \frac{y_1.\overline{y_2}-y_2.\overline{y_1}}{y_2-y_1}, \\ &\text{if } y_2 < y \leq 100, && y_{new} = \frac{100-\overline{y_2}}{100-y_2}.y + \frac{y_2.100-100.\overline{y_2}}{100-y_2}, \end{aligned} \quad (2)$$

In the next section, this reparameterization is applied to a group of ten subjects after anatomical landmark detection.

III. EXPERIMENTS

Ten right-handed healthy subjects (mean 27.5 y.o.) underwent a block-design fMRI protocol while performing 2 different movements (extension / flexion), with the thumb of both hands (right dominant / left non-dominant), each separately. Due to paper length limitation, left thumb movements and consequently right CS, were not considered. During task and rest periods, BOLD functional images were acquired with a high spatial resolution of $1.5\times1.5\times1.5$ mm^3 obtained using a multi-shot EPI sequence on a 3T whole-body MR scanner (Bruker, Medspec S300). The acquisition volume comprised 15 1.5mm-thick slices covering the upper part of the brain containing the hand knob, with a repetition time of 6 seconds. A total of 222 functional volumes were acquired during 4 functional runs. T1-weighted structural images were acquired with $1\times1\times1$ mm^3 spatial resolution using a MDEFT sequence. Anatomical images were processed through the BrainVisa T1 Pipeline[2], in order to extract the left CS mesh. Each mesh was parameterized [3], then sulcal profile was computed, L_1 and L_2 detected and the mesh reparameterized. Meshes were finally resampled using the parameterization in order to provide an inter-subject node-to-node matching. This inter-subject matching was used to compute a mean left CS for the group of subject (Fig. 6).

Functional images were processed using SPM8[3] for realignment, slice-timing, and co-registration with anatomy. A trilinear interpolation was then performed to compute functional information at each node of the left CS mesh. Finally, a surface-based statistical t-map was computed for each subject by computing a GLM over the surface [6]. Using the node-to-node inter-subject matching, a Random Effect (RFX) group map [7] was also computed on the mean CS.

IV. RESULTS AND DISCUSSION

A. Anatomical inter-subject matching

On the 10 subjects, we found average positions of the two landmarks at $\overline{y_1} = 41$ and $\overline{y_2} = 54$. A visual inspection of the results showed that L1 and L2 were properly detected on all 10 subjects and reparameterization was performed using these average values.

The sulcal profiles of the 10 subjects before and after reparameterization are shown in Fig. 4. The variability of localization of the two landmarks is visible before reparameterization. Indeed y_1 varies between positions 32 and 47, and y_2 varies between positions 44 and 62. The good match of both landmarks is visible after reparameterization.

[2]http://brainvisa.info
[3]http://www.fil.ion.ucl.ac.uk/spm

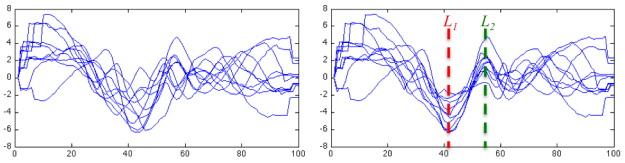

Fig. 4. Sulcal profiles of the ten subjects before (left) and after (right) reparameterization.

This effect also has consequences when using the inter-subject matching provided by the parameterization of the sulcus. When used to compute a mean CS, the quality of this inter-subject matching can be assessed. Fig. 6 shows the mean CS before and after reparameterization. After reparameterization the match of $L1$ and $L2$ is such that the knob has preserved its shape and appears clearly despite the effect of the averaging. Before parameterization , on the other hand, the variations of sulcal profile have been partly smoothed out.

Interestingly, the improvement does not only concern the bent part of the sulcus between L_1 and L_2 but also other features of the sulcus. The mean sulci and the corresponding sulcal profiles on Fig. 6 show that the curved part of the sulcus after L_2, very often present on individuals (see Fig. 3), is preserved on the mean SC only after reparameterization. The PPFM, a depth-related landmark that is not taken into account by the reparameterization process, is also better matched across subject. Fig. 5 shows the mean depth curve before and after reparameterization. The decrease of depth corresponding to the PPFM between SP and IP is a lot clearer after reparameterization.

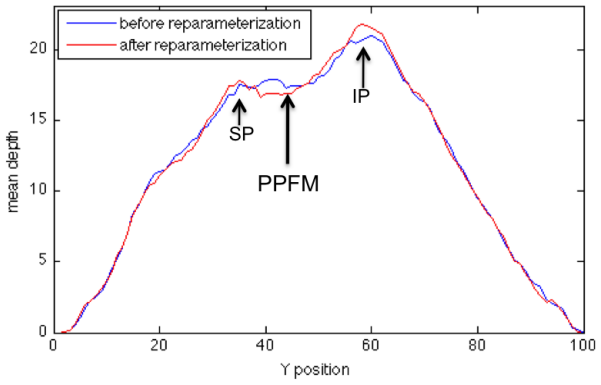

Fig. 5. Mean depth curve. The PPFM is better defined after reparameterization.

These elements show a overall better matching of CS morphology across subjects when explicitly taking into account L_1 and L_2.

B. Link with primary motor functions of the hand

Individual statistical maps were first computed on the CS mesh of each subject. A search for maxima after a threshold at $p < 0.001$ uncorrected, a standard threshold, showed that 9 out of the 10 subjects had activation peaks located

between L_1 and L_2. The tenth subject, with an overall poorer functional response, also had two activation peaks between L_1 and L_2 but just below the threshold. This link between the thumb primary motor activation and our two landmarks is confirmed by the RFX group analysis. On Fig. 6 one can see the results of this RFX analysis, thresholded at $p < 0.001$ uncorrected, before and after reparameterization. Due to the variability of the primary motor focus along the CS, the RFX analysis yielded no significant result. The RFX after reparameterization, on the other hand, showed a clear activation focus between L_1 and L_2 with a very strong significance ($p < 2.10^{-5}$)

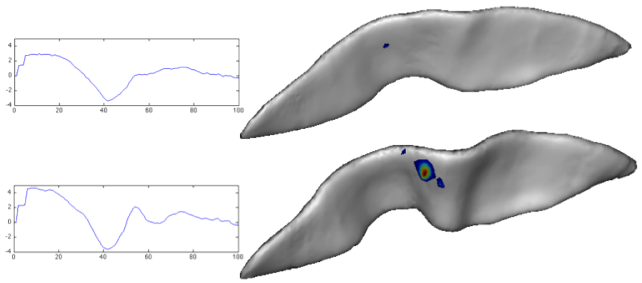

Fig. 6. Mean left central sulcus with RFX map thresholded at $p < 0.001$ uncorrected, before (top) and after reparameterization (bottom). Corresponding sulcal profiles are shown on the left. The effects of the reparameterization is visible with thumb related activations surviving the threshold and a mean anatomy that has better preserved morphological features.

This shows the strong link between anatomical landmarks L_1 and L_2 and the hand-related primary motor area in M1.

V. CONCLUSION

Based on the parameterization of each individual central sulcus, we defined two specific landmarks L_1 and L_2 that seem stable across healthy individuals. We provided an automatic detection method for these landmarks after introducing a new morphological characteristic for the central sulcus, the sulcal profile. These landmarks are used for the computation of a new parameterization of individual central sulci and the constitution on an anatomically-based common referential where individual functional activations can be accurately localized. Clearly, our study demonstrates that such a parameterization has a direct and strong impact at the group-level on functional activation detection. The implications of such process are manifold. From the functional point of view, the proposed CS parameterization allows us to study in depth, in healthy volunteers, the cortical representation of various hand movements (fingers and wrists). Pathological hand movement, after surgery or rehabilitation could be explored in this context to support a theory of adult brain plasticity. From an anatomical point of view, L_1 and L_2 provides more information to pursue studies such as those presented in [3], [4] and investigate possible morphologies of the CS. Finally, the link between morphology and function can be studied by investigating the correlation between functional specificities such as handedness and left/right CS asymmetries measured with the positions of L_1 and L_2.

VI. ACKNOWLEDGMENTS

O. Coulon is funded by the Agence Nationale de la Recherche (ANR-09-BLAN-0038-01, 'BrainMorph')

REFERENCES

[1] T.A. Yousry, U.D. Schmid, H. Alkadhi, D. Schmidt, A. Peraud, A. Buettner, P. Winkler, Localization of the motor hand area to a knob on the precentral gyrus. A new landmark, *Brain*, vol. 120 (Pt 1), 1997, pp 141-157.

[2] P. Broca, Mémoires d'anthropologie, Paris: Reinwald, 1888.

[3] M.D. Cykowski, O. Coulon, P.V. Kochunov, K. Amunts, J.L. Lancaster, A.R. Laird, D.C. Glahn, P.T. Fox, The central sulcus: an observer-independent characterization of sulcal landmarks and depth asymmetry, *Cerebral Cortex*, vol. 18(9), 2008, pp 1999-2009.

[4] W. Hopkins, O. Coulon, J.-F. Mangin, Observer-Independent Characterization of Sulcal Landmarks and Depth Asymmetry in the Central Sulcus of the Chimpanzee Brain, *Neuroscience*, vol. 171(2), 2010, pp 544-551.

[5] A. Roche, P.-J. Lahaye, J.-B. Poline, Incremental Activation Detection in fMRI Series using Kalman Filtering. *In Proc. 2nd IEEE ISBI, Arlington, VA*, 2004, pp 376-379.

[6] S.Kiebel, A.J. Holmes, ?The general linear model, *In Human Brain Function, Chap. 7, Academic Press*, 2004.

[7] W.D. Penny, A.J. Holmes, Random Effects Analysis, *In Human Brain Function, Chap. 12, Academic Press*, 2004.